

Far-infrared transmittance and reflectance studies of oriented $\text{YBa}_2\text{Cu}_3\text{O}_{7-\delta}$ thin films

F. Gao, G. L. Carr,* C. D. Porter, and D. B. Tanner

Department of Physics, University of Florida, Gainesville, Florida 32611

S. Etemad, T. Venkatesan, and A. Inam

Bell Communications Research, Red Bank, New Jersey 07701

B. Dutta and X. D. Wu

Department of Physics, Rutgers University, Piscataway, New Jersey 08855

G. P. Williams and C. J. Hirschmugl

Brookhaven National Laboratory, Upton, New York 11973

(Received 3 August 1990)

We have measured both the transmittance (\mathcal{T}) and reflectance (\mathcal{R}) for several $\text{YBa}_2\text{Cu}_3\text{O}_{7-\delta}$ thin films over the frequency range from 20 to 360 cm^{-1} at temperatures between 20 and 300 K. The films, grown on MgO substrates by pulsed laser ablation, are highly a - b -plane oriented. We use \mathcal{T} and \mathcal{R} to extract the optical conductivity, and find good agreement with results from Kramers-Kronig analysis of reflectance measurements alone. The transmittance is consistent with a two-component dielectric function consisting of Drude (free-carrier) and midinfrared (bound-carrier) absorption. The Drude relaxation rate varies linearly with temperature, and compares well with values obtained from the measured dc resistivity. We use a two-fluid model for the superconducting state and obtain a BCS-like temperature dependence for the superfluid density. A superconducting gap is not observed in our spectra.

I. INTRODUCTION

The infrared properties of the high- T_c superconductors continue to receive considerable attention.¹⁻¹⁸ Most of the work to date determines the frequency-dependent conductivity through Kramers-Kronig analysis of reflectance measurements.¹⁻¹¹ A few transmittance measurements have been made,¹²⁻¹⁴ as well as a direct absorption measurement.¹⁵ In many studies, the normal state of ceramics, crystals, and thin films have been described by a two-component model, consisting of temperature-dependent free-carrier absorption (Drude part) and a broad, nearly temperature-independent electronic excitation (midinfrared absorption).^{2-4,9-12} This approach has been adopted because it is clear that a single, strongly damped, Drude term, used to model the infrared data in many early measurements, does not work.¹ An alternative single-component picture—called “marginal Fermi liquid”¹⁹ and “nested Fermi liquid”²⁰—has also been put forward. In this approach there is only a single type of charge carrier; strong frequency-dependent scattering from a broad range of optically inactive excitations leads in the midinfrared region to a temperature-independent conductivity while at low frequencies (including dc) the conductivity goes inversely with the temperature. In this paper, we adopt the two-component picture in modeling our data for several reasons. First, the data do not extend to high enough frequency to enable a critical comparison of the two approaches. In addition, as shown below, the measurements at high temperatures show qualitative difference to the single-

component picture. Finally, the two-component picture allows us to discuss the behavior below T_c in a quantitative way. In the superconducting state, according to the two-component picture, the Drude oscillator strength collapses to a δ function at the origin.

Attempts have been made^{1,3(a),5-7,16,17} to assign the superconducting energy gap either to the edge of a rapid drop in the ratio R_s/R_n of superconducting to normal reflectance or to the absorption onset of the conductivity σ_{1s} . The values of $2\Delta(0)/k_B T_c$ obtained in this way range between 2.5 and 8. There has been a controversy, however, whether these structures are due to the energy gap or are part of the midinfrared absorption.^{4,9-11,3(b),18}

In this paper, we present the results of a detailed study of the far-infrared properties of three $\text{YBa}_2\text{Cu}_3\text{O}_{7-\delta}$ thin films. In agreement with earlier studies, we find a nearly temperature-independent non-Drude absorption in the far-infrared region below 300 cm^{-1} . The temperature dependence of the normal-state Drude parameters agrees with the independently measured dc resistivity of the same sample. Using a two-fluid model to fit the transmission data in the superconducting state, we observe that the Drude contribution, which is still present, drops rapidly with decreasing temperature, suggesting that the normal carriers responsible for the dc transport condense rapidly into a superfluid state. The low-frequency tail of the midinfrared band remains for $T \ll T_c$.

II. EXPERIMENT

The films were prepared by pulsed-laser ablation from a stoichiometric target.²¹ The films, grown on 1-mm-

thick MgO, are highly oriented with the c axis normal to the surface. Other commonly used substrates for high- T_c superconducting films are SrTiO₃, LaAlO₃, LaGaO₃, and yttria-stabilized zirconia. None of these are transparent through the far-infrared region, thus they are not suitable for transmission studies of thin films. In contrast, MgO is reasonably transparent up to 330 cm⁻¹ at low temperatures and at the same time is suitable for oriented growth. Hence it is the best choice as a substrate for far-infrared transmission studies of high- T_c films. The characteristics of our samples are listed in Table I. The table gives the film thickness, transition temperature T_c , transition width ΔT_c , and measured four-probe room-temperature conductivity. Film thicknesses for two films (480 and 1560 Å) were measured by Rutherford backscattering (RBS) and step profilometry. The two techniques agreed to within 100 Å. Film thickness for the 1800-Å film was estimated from growth conditions.

The samples were mounted on a helium-cooled cold finger with a calibrated diode thermometer mounted nearby. The films, with surface dimensions of 5 × 5 mm², were circularly masked to reduce their areas to about 4 mm diameter. Transmittance spectra from 20 to 100 cm⁻¹ for the 480- and 1560-Å films, and 20–375 cm⁻¹ for the 1800-Å film, were measured using the far-infrared beamline at the National Synchrotron Light Source (NSLS).²² Transmittance spectra over 50–375 cm⁻¹ for the 480- and 1560-Å films and reflectance over 20–375 cm⁻¹ for all three films were measured using a Bruker Fourier-transform interferometer with a Hg arc lamp source and 4.2-K bolometer detector. The infrared radiation was incident normal to the films so that the electric field was in the a - b plane of the films. Sample and reference spectra were measured three times each to estimate the random noise.

We focused our attention on the far-infrared region below 350 cm⁻¹ since the MgO substrate is opaque just above 350 cm⁻¹ at all temperatures due to a TO-phonon mode near 400 cm⁻¹.²³ To average over interference fringes due to multiple internal reflections in the substrate, the measurements were made at relatively low resolution ($\Delta\omega = 20$ cm⁻¹ or so) and interpolated to give smooth curves. In addition, we carefully measured both the reflectance \mathcal{R}_{sub} and transmittance \mathcal{T}_{sub} of a bare MgO substrate at each temperature where film data were taken. \mathcal{T}_{sub} is shown in Fig. 1. It is reasonably high below 300 cm⁻¹ for $T \leq 100$ K, reaching nearly 60% and with almost no absorption below 100 cm⁻¹. There is structure near 100, 155, and 290 cm⁻¹ caused by multiphonon processes.²³ At higher temperatures, phonon difference processes cause absorption below the TO-

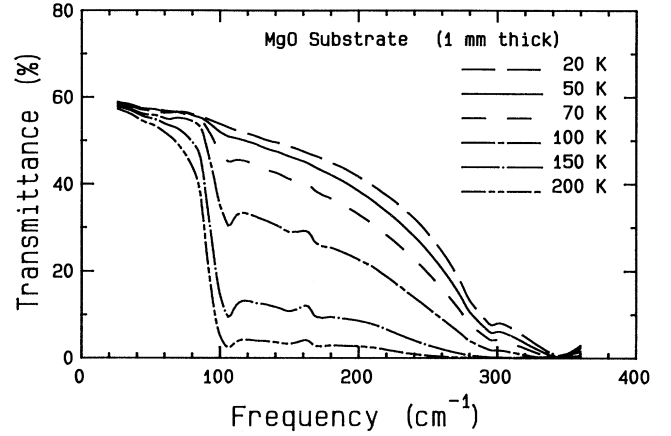


FIG. 1. Transmittance of MgO at selected temperatures between 300 and 20 K.

phonon frequency. This absorption also affects the transmittance of the YBa₂Cu₃O_{7- δ} /MgO samples. To account for substrate absorption, the frequency-dependent absorption coefficient α and index of refraction n of the MgO were determined by solving $\mathcal{R}_{\text{sub}}(\alpha, n)$ and $\mathcal{T}_{\text{sub}}(\alpha, n)$. These measurements were then used in analysis of the data for the films.

III. CONDUCTIVITY EXTRACTION

For a film of thickness $d \ll \lambda$, the wavelength of far-infrared radiation, and $d \ll \lambda_L, \delta$, the penetration depth, the film may be treated as a sheet of conductor of complex admittance $y = y_1 + iy_2$. In this case, the transmission through, \mathcal{T}_f , and reflection from, \mathcal{R}_f , a film on a substrate with index n are

$$\mathcal{T}_f = \frac{4n}{(y_1 + n + 1)^2 + y_2^2}, \quad (1)$$

and

$$\mathcal{R}_f = \frac{(y_1 + n - 1)^2 + y_2^2}{(y_1 + n + 1)^2 + y_2^2}. \quad (2)$$

These single-layer equations are generalizations of expressions given by Glover and Tinkham.²⁴ The dimensionless complex admittance of the thin film is related to the conductivity σ by $y = Z_0 d \sigma$ or $y_1 + iy_2 = Z_0 d (\sigma_1 + i\sigma_2)$. Here, d is the film thickness and $Z_0 = 377 \Omega = 4\pi/c$ (esu) is the impedance of free space. For a nearly opaque metal film, the total reflectance of film plus substrate is $\mathcal{R} \approx \mathcal{R}_f$. Equation (1) gives the transmission across the film into the substrate. This quantity is related to the measured transmittance \mathcal{T} by

$$\mathcal{T} = \frac{(1 - \mathcal{R}_s) e^{-\alpha x}}{1 - \mathcal{R}_s \mathcal{R}'_f e^{-2\alpha x}} \mathcal{T}_f, \quad (3)$$

where x is the thickness and α the absorption coefficient of the substrate. The other terms in Eq. (3) are the substrate-incident internal reflection of the film,

TABLE I. Sample characteristics.

Thickness (Å)	T_c (K)	ΔT_c (K)	σ_{dc} (at 300 K) ($\Omega^{-1} \text{cm}^{-1}$)
1800	89	2	~2000
1560	90	1	2500
480	83	3	1600

$$\mathcal{R}'_f = \frac{(y_1 - n + 1)^2 + y_2^2}{(y_1 + n - 1)^2 + y_2^2},$$

and the single bounce reflection of the substrate,

$$\mathcal{R}_s \approx \left(\frac{n-1}{n+1} \right)^2,$$

when $k \equiv c\alpha/2\omega \ll n$ as is the case here. Equation (3) assumes a thick or wedged substrate, so that there is no coherence among multiple internal reflections within the substrate.

After measuring \mathcal{T} and \mathcal{R} at each frequency, we determined y_1 and y_2 , and hence σ_1 and σ_2 by inverting Eqs. (1)–(3). In this procedure we used the values of α and n measured for the substrate, and iterated for a self-consistent \mathcal{R}'_f .

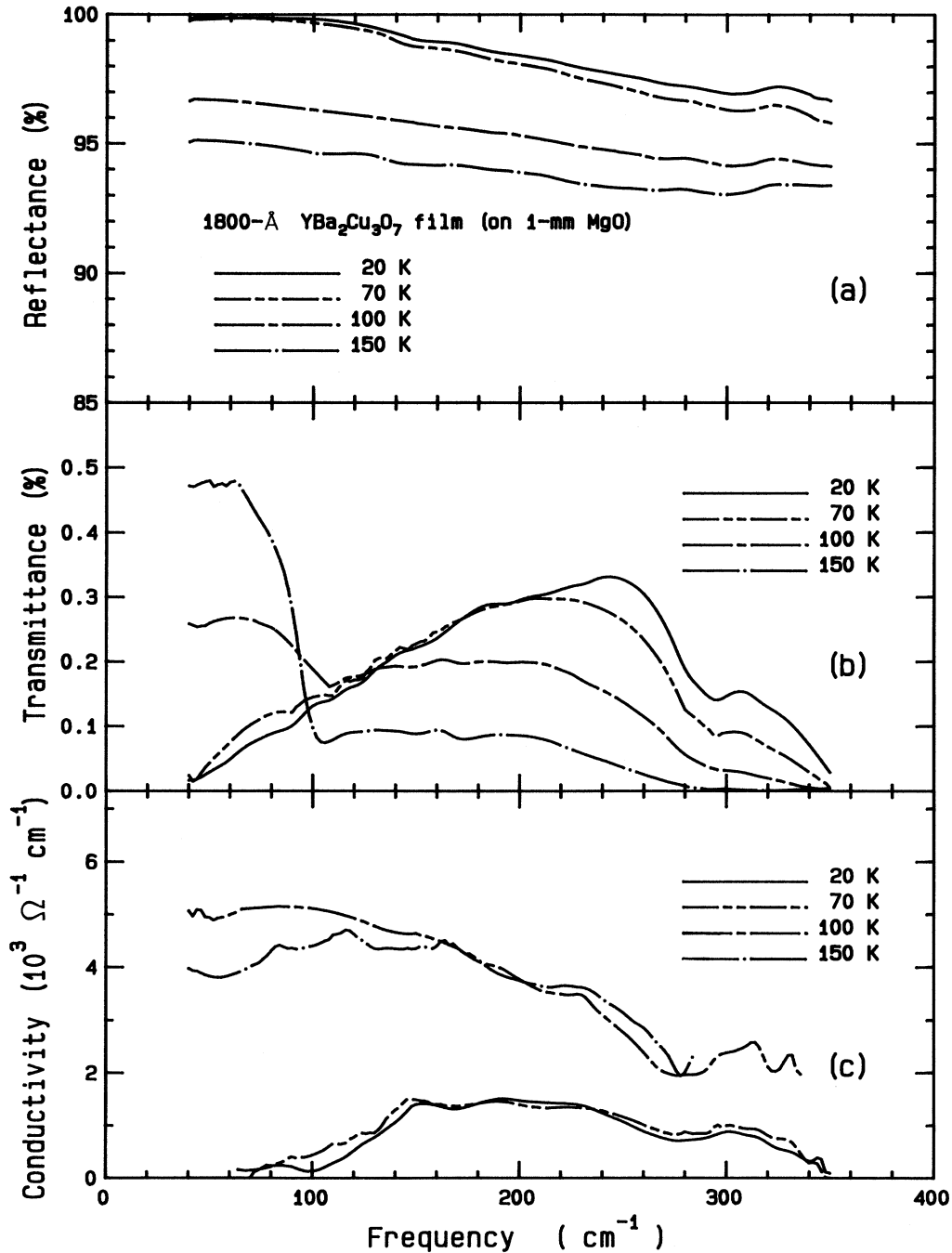


FIG. 2. (a) Measured far-infrared reflectance, (b) transmittance, (c) and optical conductivity obtained from \mathcal{R} and \mathcal{T} of 1800-Å-thick $\text{YBa}_2\text{Cu}_3\text{O}_{7-8}$ film deposited on a 1-mm-thick MgO substrate.

IV. RESULTS AND DISCUSSION

The upper and middle panels of Fig. 2 show, respectively, the reflectance and transmittance of a 1800-Å $\text{YBa}_2\text{Cu}_3\text{O}_7$ film on MgO. The reflectance is well below unity in the normal state at all frequencies. It is greatly enhanced in the superconducting state and very nearly 100% for frequencies below 150 cm^{-1} . The *a-b*-plane phonons, strongly screened by free carriers, are not visible and the *c*-axis phonons are not probed since we are sensing solely *a-b*-plane response.^{16,17} The \mathcal{T} spectra are complicated by the MgO substrate which must be dealt with properly to extract the frequency-dependent optical conductivity. However, the transmittance approaches zero at low frequencies for $T < T_c$, as expected for a superconductor.

The bottom panel of Fig. 2 is the conductivity derived from \mathcal{R} and \mathcal{T} . In the normal state, the conductivity is nearly equal to the dc conductivity at low frequencies but has a non-Drude (midinfrared) contribution at higher frequencies. Below T_c , when the Drude part condenses, the remaining conductivity—with overall level of $1500\text{ }(\Omega\text{ cm})^{-1}$ —can be attributed to the low-frequency part of the midinfrared absorption. These results are similar to those previously obtained by Kramers-Kronig analysis of reflectance.^{2–10}

The conductivity we obtain in the superconducting state has large errors below 150 cm^{-1} , because the reflectance is nearly 100%. The conductivity is $\sigma_1 = (cn/4\pi d)(1 - \mathcal{R}_f - \mathcal{T}_f)/\mathcal{T}_f$. As $\mathcal{R}_f \rightarrow 1 \pm \text{noise}$, the accuracy of the conductivity becomes small, with systematic error in the reflectance level becoming dominant in the conductivity extraction. Once the errors in \mathcal{R} are comparable to the magnitude of \mathcal{T} , the method breaks down completely. This is the case below T_c for most of our measurements. The use of \mathcal{R} and \mathcal{T} to find σ_1 is most accurate when $\mathcal{R} \approx \mathcal{T} < 0.5$. For this condition to hold, we would need $\sim 50\text{-Å}$ films. (A similar problem occurs in Kramers-Kronig analysis of highly reflecting bulk samples.⁹) Thus, in the remainder of this paper we will emphasize transmittance data.

Figure 3 shows the “free-standing” transmittance, calculated from Eq. (1) for three films at temperatures between 20 and 200 K. (The 1800-Å film is the same as shown in Fig. 2.) The absorption and dispersion in the substrate have been removed in these curves; the refractive index has been set to $n = 1$. Note that the data below T_c extrapolate to zero, indicating that the inductive response of the superconductor dominates at these frequencies, as expected. At the higher temperatures, the slope of \mathcal{T}_f changes sign; the transmittance decreases with increasing frequency. This behavior is consistent with a two-component (Drude plus midinfrared) infrared conductivity but is inconsistent with either simple Drude behavior or with a generalized Drude conductivity having a frequency-dependent scattering rate of the form $1/\tau = \max(\omega, k_B T/\hbar)$. This latter dependence has been suggested by models of marginal Fermi liquids¹⁹ and nested Fermi liquids.²⁰ If the admittance is large (the case here, where $\mathcal{T}_f \ll \mathcal{T}_{\text{sub}}$), then $\mathcal{T}_f \propto (1/|\sigma|^2)$ or

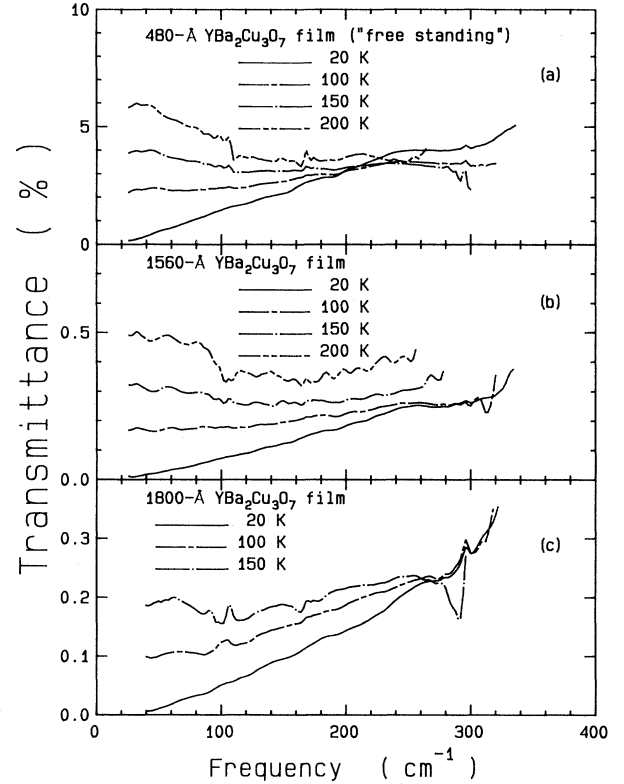


FIG. 3. Free-standing far-infrared transmittance of three $\text{YBa}_2\text{Cu}_3\text{O}_{7-\delta}$ films at temperatures between 20 and 200 K.

$$\mathcal{T}_f = 4n(c/d)^2 \frac{1/\tau^2 + \omega^2}{\omega_p^4}, \quad (4)$$

where ω_p is the plasma frequency and $1/\tau$ is the free-carrier scattering rate. Whether $1/\tau$ is constant or increasing with ω , the transmittance will increase with ω , in disagreement with the higher-temperature data of Fig. 3.

In a two-component picture, the decreasing transmittance is a consequence of the midinfrared absorption. At high temperatures, the Drude absorption is quite broad and overlaps the midinfrared band. Thus, as ω increases, the total conductivity (Drude plus midinfrared) increases and \mathcal{T}_f decreases.

We have used simple models^{2–4,9} for the two components in order to fit the transmittance data. In the normal state, the dielectric function is a sum of a narrow Drude band, broad midinfrared Lorentzians, and high-frequency contribution:

$$\begin{aligned} \epsilon(\omega) &= -\frac{\omega_p^2}{\omega^2 + i\omega/\tau} + \sum_{j=1}^2 \frac{\omega_{pj}^2}{\omega_j^2 - \omega^2 - i\omega\gamma_j} + \epsilon_\infty \\ &= \epsilon_{\text{Drude}} + \epsilon_{\text{mid-ir}} + \epsilon_\infty \quad (T > T_c), \end{aligned} \quad (5)$$

where ω_{pj} , ω_j , and γ_j are the oscillator strength, center frequency, and width of the *j*th Lorentzian band in $\epsilon_{\text{mid-ir}}$ and ϵ_∞ is the contributions from absorption at frequencies above $\sim 1000\text{ cm}^{-1}$.

In the superconducting state, to accommodate temperatures near T_c , we assumed the Drude contribution remains due to some fraction of nonsuperconducting carriers. Thus, we tried a two-fluid model:

$$\epsilon(\omega) = (1 - f_s)\epsilon_{\text{Drude}} + f_s\epsilon_{\text{sup}} + \epsilon_{\text{mid-ir}} + \epsilon_{\infty} \quad (T < T_c), \quad (6)$$

where ϵ_{Drude} , $\epsilon_{\text{mid-ir}}$, and ϵ_{∞} are the same as those in Eq. (5), f_s is the fraction of the free-carrier electron density in the superfluid, and

$$\epsilon_{\text{sup}} = -\frac{\omega_p^2}{\omega^2} + i\frac{\pi\omega_p^2}{2\omega}\delta(\omega). \quad (7)$$

The details of the fit are rather complicated because of the many parameters. We have tried to reduce these to as few as possible, particularly the temperature-dependent ones. Because the data extend only to 350 cm^{-1} , we fixed the parameters for the higher mid-ir oscillator at center frequency $\omega_2 = 720 \text{ cm}^{-1}$, strength $\omega_{p2} = 10000 \text{ cm}^{-1}$, and width $\gamma_2 = 1400 \text{ cm}^{-1}$ as suggested by Ref. 9. In addition, we fixed $\epsilon_{\infty} = 25$. Then we varied the Drude parameters ω_p and $1/\tau$ as well as the fraction f_s and the lower mid-ir oscillator, at $\omega_1 \approx 200 \text{ cm}^{-1}$. In other words, we varied six parameters (ω_p , $1/\tau$, f_s , ω_1 , ω_{p1} , and γ_1). However, we found that we could obtain good fits by making ω_p , ω_{p1} , and ω_1 temperature independent. For the 480-Å film, $\omega_p = 7700 \text{ cm}^{-1}$, $\omega_{p1} = 9900 \text{ cm}^{-1}$, $\omega_1 = 200 \text{ cm}^{-1}$, and $\gamma_1 = 750 \text{ cm}^{-1}$. For the 1560-Å film, $\omega_p = 10000 \text{ cm}^{-1}$, $\omega_{p1} = 9700 \text{ cm}^{-1}$, $\omega_1 = 280 \text{ cm}^{-1}$, and $\gamma_1 = 700 \text{ cm}^{-1}$. Finally, for the 1800-Å film, $\omega_p = 9400 \text{ cm}^{-1}$, $\omega_{p1} = 7800 \text{ cm}^{-1}$, $\omega_1 = 200 \text{ cm}^{-1}$, and $\gamma_1 = 700 \text{ cm}^{-1}$. We attribute the difference in oscillator strengths among the films in part to uncertainties in the film thickness. Because the transmittance is governed by $y = Z_0 d \sigma$, errors in d give equal errors in ω_p^2 and ω_{p1}^2 .

Figure 4 shows the transmittance raw data (as dots, with a symbol on every 20th point for identification purposes) of a 480-Å film at selected temperatures. The solid curves are model fits. It appears the models give excellent fits to the experimental data both in the normal and superconducting states. We also found that the relaxation rate for $T > T_c$ was linear in temperature, $1/\tau \approx 2.8k_B T$, with nearly zero intercept. Below T_c the two-fluid model gave a rather sudden drop in $1/\tau$ near T_c , with saturation at $T \approx 50 \text{ K}$ and below.

Figure 5(a) shows the temperature dependence of $1/\tau$ above T_c . This is compared with $(1/\tau)_{\text{dc}}$ determined from the measured four-probe dc resistivity ρ_{dc} according to

$$(1/\tau)_{\text{dc}} = \frac{\omega_p^2}{4\pi}\rho_{\text{dc}}, \quad (8)$$

where ω_p is the plasma frequency from the fit to \mathcal{T} . The magnitude of $(1/\tau)_{\text{dc}}$ is about 30% higher than that of the far-infrared (FIR) relaxation rate $(1/\tau)_{\text{FIR}}$. We note that the slopes of the two determinations are nearly the same; it is the $T=0$ intercept which is larger in the dc

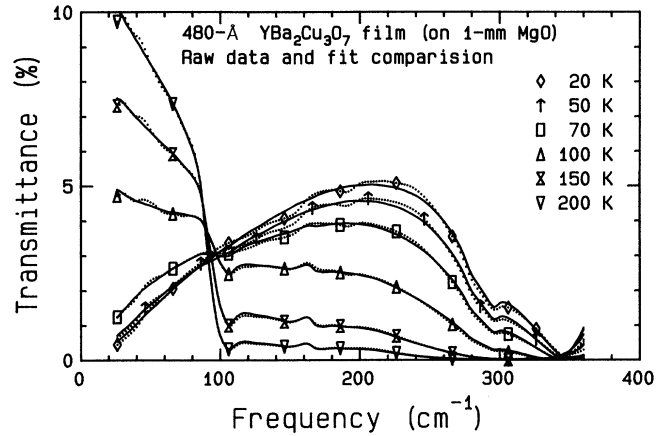


FIG. 4. Measured transmittance (in dots and symbols) of a 480-Å $\text{YBa}_2\text{Cu}_3\text{O}_{7-\delta}$ film deposited on a 1-mm-thick MgO substrate at selected temperatures above and below T_c . The solid curves are fit to the data using a two-component model for the dielectric function.

case. Taking $v_F = 2 \times 10^7 \text{ cm/sec}$, and using our relaxation rate of $1/\tau \approx 180 \text{ cm}^{-1}$ at 100 K, we can estimate the mean free path $l = v_F \tau = 60 \text{ Å}$.

Figure 5(b) shows the temperature dependence of the superfluid electron density fraction $f_s(T)$. This

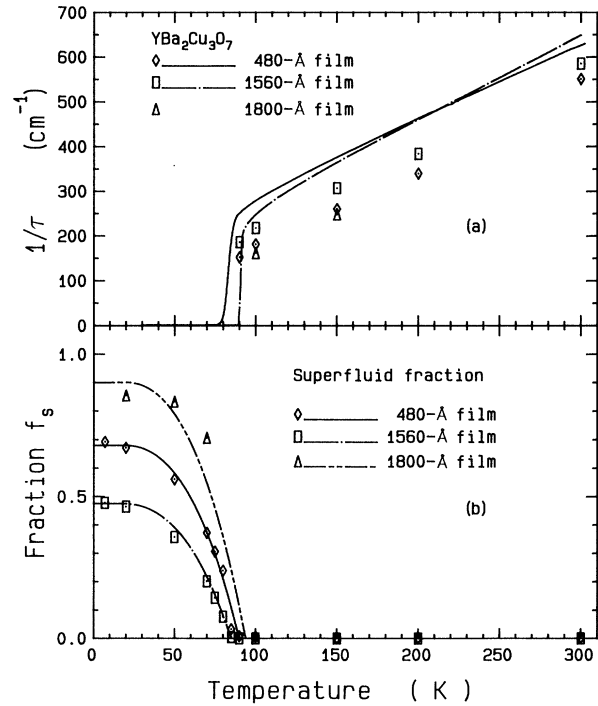


FIG. 5. (a) Temperature dependence of Drude scattering rate, $1/\tau$, obtained from fits to the transmittance (in symbols) and estimated from dc resistivity (in solid and dash-dotted lines). (b) superfluid density, $f_s(T) \equiv n_s(T)/n$, vs temperature. The curves are $f_s(T)$ as predicted by the BCS theory, taking $f_s(0) = 0.68$ (480 Å), 0.47 (1560 Å), and 0.90 (1800 Å).

quantity—which essentially is a measure of the strength of the zero-frequency δ function in $\sigma_1(\omega)$ —dominates and is determined by the low-frequency behavior of the transmittance. As can be seen in Fig. 4, T changes substantially through the superconducting transition with even a sign change in the slope of the curve. Thus, despite the relatively large number of parameters in our model, the quantity f_s is well determined by the data. Note that $f_s = 0$ above T_c . Below T_c , the normal carriers condense rapidly into the superfluid; hence, f_s increases as temperature drops. The curves in Fig. 4(b) correspond to the behavior of $f_s(T)$ in BCS theory,

$$f_s = f_{s0} \left[\frac{\Delta(T)}{\Delta_0} \right]^2, \quad (9)$$

where f_{s0} is the zero-temperature value, $\Delta(T)$ is the temperature-dependent BCS order parameters, and Δ_0 its $T=0$ value. Although f_s never reaches 1, it appears that this two-fluid model gives otherwise a good description of the temperature dependence of the order parameter. We are unable to determine whether the ~ 30 – 50% remaining Drude oscillator strength in the two thinner films is due to a defective layer or is intrinsic to the material.

In contrast to $1/\tau$, the midinfrared band has very little temperature dependence, in agreement with the similar results reported from reflectance measurements.⁹ We noticed that the overall size and shape of the midinfrared contribution to the conductivity remained almost unchanged at all temperatures.

Finally, there is no evidence in our spectra for a superconducting gap in the 50 – 300-cm^{-1} region at any temperature. This is illustrated in Fig. 6, which shows the free-standing transmittance for our 480-\AA film for four temperatures below T_c . In an ordinary superconducting film,^{24,25} the transmission increases up to the gap energy 2Δ , where there is a maximum followed by a drop at higher frequencies, due to the increasing $\sigma(\omega)$ above the gap. No such structure is seen in our data. This can be understood within a “clean-limit” picture;⁹ the relaxation rate of the free carriers is $\sim 200\text{ cm}^{-1}$ at 100 K , smaller than the gap expected for a $T_c = 90\text{ K}$, BCS superconductor. Thus most of the free-carrier oscillator strength is at frequencies below 2Δ , leaving little strength for transitions across the gap. Any remaining structure is masked by the tail of the midinfrared absorption.

To show the effect of a gap in the intermediate limit, we have calculated the transmittance within the Leplae²⁶ model for our 480-\AA film. This is shown as the solid line in Fig. 6. The parameters used in the calculation were $\omega_p = 7700\text{ cm}^{-1}$ (from the two-component model fit discussed above), $2\Delta = 225\text{ cm}^{-1}$, and $1/\tau = 100\text{ cm}^{-1}$. With these parameters, the calculated transmittance is systematically higher than the measurement. In the intermediate limit, oscillator strength is removed from the zero-frequency δ function and put into the gap transition. This reduces σ_2 and increases the calculated transmittance. The calculation could be brought back down to

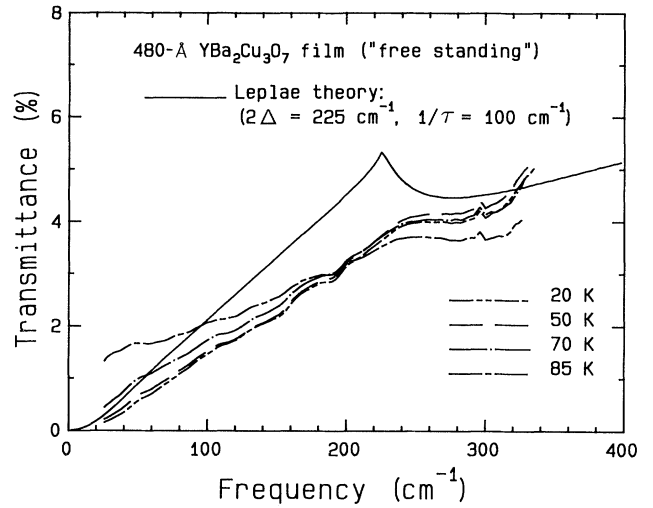


FIG. 6. Free-standing transmittance of the 480-\AA film below T_c . The solid curve is a calculation from the Leplae model.

the measured transmittance with an increase in ω_p ; however, this would lead to a significant difference in free-carrier oscillator strength above and below T_c .

The calculation shows a sharp upwards cusp in the transmittance which is reproduced neither in these data nor in the results of others.^{12,13} As temperature is increased, the cusp in the calculation would weaken and shift to lower temperatures as the value of the T -dependent gap decreased. No such shift is observed in our measurement. Thus our transmission data are more consistent with a clean-limit picture than with an intermediate or dirty-limit picture.

V. CONCLUSIONS

Far-infrared transmittance and reflectance spectra for $\text{YBa}_2\text{Cu}_3\text{O}_{7-\delta}$ thin films show a Drude response and midinfrared absorption in the frequency range below 350 cm^{-1} . In transmittance fits, the Drude relaxation rate is linear T in the normal state while the plasma frequency is essentially constant. The mid-ir absorption, in contrast, is nearly temperature independent both for $T > T_c$ and for $T < T_c$. The two-fluid model works for our samples and implies a BCS-like temperature dependence of the condensate fraction; however, $f_s < 1$ in our samples. The films are near the clean limit and no distinct gap feature has been found in the frequency range below 350 cm^{-1} .

ACKNOWLEDGMENTS

Research at the University of Florida is supported by the U. S. Defense Advanced Research Projects Agency Grant No. MDA-972-88-J-1006. NSLS is supported by the Department of Energy through Contract No. DE-AC02-76CH00016.

- *Present address: Corporate Research Center, Grumman Aerospace, Bethpage, NY 11714.
- ¹For a review, see T. Timusk and D. B. Tanner, in *Physical Properties of High Temperature Superconductors I*, edited by D. M. Ginsberg (World Scientific, Singapore, 1989), p. 339.
- ²D. A. Bonn, A. H. O'Reilly, J. E. Greedan, C. V. Stager, T. Timusk, K. Kamarás, and D. B. Tanner, *Phys. Rev. B* **37**, 1574 (1988).
- ³(a) G. A. Thomas, J. Orenstein, D. H. Rapkine, M. Capizzi, A. J. Millis, R. N. Bhatt, L. F. Schneemeyer, and J. V. Waszczak, *Phys. Rev. Lett.* **61**, 1313 (1988); (b) S. L. Cooper, G. A. Thomas, J. Orenstein, D. H. Rapkine, M. Capizzi, T. Timusk, A. J. Millis, L. F. Schneemeyer, and J. V. Waszczak, *Phys. Rev. B* **40**, 11358 (1989).
- ⁴T. Timusk, S. L. Herr, K. Kamarás, C. D. Porter, D. B. Tanner, D. A. Bonn, J. D. Garrett, C. V. Stager, J. E. Greedan, and M. Reedyk, *Phys. Rev. B* **38**, 6683 (1988).
- ⁵R. T. Collins, Z. Schlesinger, F. Holtzberg, and C. Field, *Phys. Rev. Lett.* **63**, 422 (1989); Z. Schlesinger, R. T. Collins, F. Holtzberg, C. Field, G. Koren, and A. Gupta, *Phys. Rev. B* **41**, 11 237 (1990); Z. Schlesinger, R. T. Collins, F. Holtzberg, C. Field, U. Welp, G. W. Crabtree, Y. Fang, and J. Z. Liu, *Phys. Rev. Lett.* **65**, 801 (1990).
- ⁶J. Schützmann, W. Ose, J. Keller, K. F. Renk, B. Roas, L. Schultz, and G. Saemann-Ischenko, *Europhys. Lett.* **8**, 679 (1989).
- ⁷S. Kamba, J. Petzelt, V. Zelezny, E. V. Pechen, S. I. Krasnosvobodtsev, and B. P. Gorshunov, *Solid State Commun.* **70**, 547 (1989).
- ⁸K. Kamarás, S. L. Herr, C. D. Porter, D. B. Tanner, T. Venkatesan, E. Chase, A. Inam, H. D. Woo, M. S. Hegde, B. Datta, and S. Etemad, in *Electronic Properties of Conjugated Polymers III*, edited by H. Kuzmany, M. Mehring, and S. Roth, Springer Series in Solid State Sciences Vol. 91 (Springer, Berlin, 1989), p.418.
- ⁹K. Kamarás, S. L. Herr, C. D. Porter, N. Tache, D. B. Tanner, S. Etemad, T. Venkatesan, E. Chase, A. Inam, X. D. Wu, M. S. Hegde, and B. Dutta, *Phys. Rev. Lett.* **64**, 84 (1990).
- ¹⁰T. Timusk, M. Reedyk, R. Hughes, D. A. Bonn, J. D. Garrett, J. E. Greedan, C. V. Stager, D. B. Tanner, F. Gao, S. L. Herr, K. Kamarás, G. A. Thomas, S. L. Cooper, J. Orenstein, L. F. Schneemeyer, and A. J. Millis, *Physica C* **162-164**, 841 (1989).
- ¹¹C. M. Foster, K. F. Voss, T. W. Hagler, D. Mihailovic, A. J. Heeger, M. M. Eddy, W. L. Olson, and E. J. Smith, *Solid State Commun.* **76**, 651 (1990).
- ¹²R. A. Hughes, T. Timusk, S. L. Cooper, G. A. Thomas, J. J. Yeh, and M. Hong, *Phys. Rev. B* **40**, 5162 (1989).
- ¹³G. P. Williams, R. C. Budhani, C. J. Hirschmugl, G. L. Carr, S. Perkowitz, B. Lou, and T. R. Yang, *Phys. Rev. B* **41**, 4752 (1990).
- ¹⁴L. F. Forro, G. L. Carr, G. P. Williams, D. Mandrus, and L. Mihaly, *Phys. Rev. Lett.* **65**, 1991 (1990).
- ¹⁵T. Pham, H. D. Drew, S. H. Moseley, and J. Z. Liu, *Phys. Rev. B* **41**, 11 681 (1990).
- ¹⁶M. K. Crawford, W. E. Farneth, R. K. Bordia, and E. M. McCarron, *Phys. Rev. B* **37**, 3371 (1988).
- ¹⁷A. Wittlin, L. Genzel, M. Cardona, M. Bauer, W. König, E. Garcia, M. Barahona, and M. V. Cabanas, *Phys. Rev. B* **37**, 652 (1988).
- ¹⁸T. Timusk and D. B. Tanner, *Physica C* **169**, 425 (1990).
- ¹⁹C. M. Varma, P. B. Littlewood, S. Schmitt-Rink, E. Abraham, and A. E. Ruckenstein, *Phys. Rev. Lett.* **63**, 1996 (1989).
- ²⁰J. Ruvalds and A. Virosztek, *Phys. Rev. B* **43**, 5498 (1991).
- ²¹X. D. Wu, D. Dijkkamp, S. B. Ogale, A. Inam, E. W. Chase, P. F. Miceli, C. C. Chang, J. M. Tarascon, and T. Venkatesan, *Appl. Phys. Lett.* **51**, 861 (1987); X. D. Wu, A. Inam, M. S. Hegde, T. Venkatesan, C. C. Chang, E. W. Chase, B. Wilkens, and J. M. Tarascon, *Phys. Rev. B* **38**, 9307 (1988).
- ²²G. P. Williams, *Nucl. Instrum. Methods Phys. Res. A* **291**, 8 (1990).
- ²³T. R. Yang, S. Perkowitz, G. L. Carr, R. C. Budhani, G. P. Williams, and C. J. Hirschmugl, *Appl. Opt.* **29**, 332 (1990).
- ²⁴R. E. Gover III and M. Tinkham, *Phys. Rev.* **108**, 243 (1957); M. Tinkham, in *Far-Infrared Properties of Solids*, edited by S. S. Mitra and S. Nudelman (Plenum, New York, 1970), p. 233.
- ²⁵D. C. Mattis and J. Bardeen, *Phys. Rev.* **111**, 412 (1958).
- ²⁶L. Leplae, *Phys. Rev. B* **27**, 1911 (1983).